Simulated effect of edge plasma density parameters on lower hybrid wave scattering in EAST

C. B. Wu,[1, 2] B. J. Ding,[1] S. G. Baek,[3] M. H. Li,[1] G. M. Wallace,[3] Y. C. Li[4] and G. H. Yan[1,2]

[1]Institute of Plasma Physics, Hefei Institutes of Physical Science, Chinese Academy of Sciences, Hefei 230031, China/P. R. China
[2]University of Science and Technology of China, Hefei 230026, China/P. R. China
[3]MIT Plasma Science and Fusion Center, Cambridge, Massachusetts 02139, USA
[4]College of Optoelectronic Engineering, Shenzhen University, Shenzhen 518060, China

Corresponding author: bjding@ipp.ac.cn

Abstract:

Incorporation of lower hybrid (LH) wave spectrum broadening in the poloidal wavenumber (k_θ) space at the last close field surface (LCFS) is reported to lead to a better agreement of the modeled LH wave current profile with the experimental results [S.G. Baek et al, *Nucl. Fusion* **61** 106034 (2021)]. To further understand its underlying mechanism and find the possible influence factors, effects of wave scattering caused by drift-wave type density fluctuation on the probability distribution of the LH wave polar refractive index (N_θ) at the LCFS are studied under density parameters in the scrape-off-layer (SOL). According to a scattering model [P. T. Bonoli and E. Ott, *Phys Fluids* **25** (2), 359-375 (1982)], scattering probability and scattering angle distribution are two main factors that determine the degree of spectral broadening. Studies presented here show that the total scattering probability increases first and then decreases as the wave propagates towards smaller normalized radius of poloidal magnetic flux (ρ). The degree of spectral broadening is found to depend on the density and density fluctuation together by changing the intensity and a proportion of the geometrical optics approximation term and the $\boldsymbol{E} \times \boldsymbol{B}$ drift term. Furthermore, the fluctuation correlation length can significantly modify the probability distribution of N_θ at the LCFS, which is found to significantly change LH wave current profile.

In the present steady-state tokamak, lower hybrid current drive (LHCD) has a number of advantages, such as control of the current density profiles[1], safety factor profile [2, 3], neoclassical tearing modes (NTMs)[4], and so on. At the same time, LHCD efficiency decreases sharply at high density[5], possibly due to strong interactions between the LH wave and the scrape-off layer (SOL)[5-10]. One possible cause is wave scattering induced by density fluctuation, which has been studied in both simulation[11-17] and experiment. The study on Alcator C-Mod suggested that drift-wave type density fluctuation can either enhance or inhibit the penetration of LH wave[18]. The study on Tore Supra showed that the time averaged LH current density profile is only slightly broader and shifted inwards by the effect of fluctuation[19]. And some studies on FTU

indicated that the SOL parameters will reduce LHCD[20], but it is difficult to distinguish between wave scattering and parametric decay instability (PDI)[6, 10]. While according to recent results[21-24], the effects of wave scattering on LH spectrum broadening at the LCFS can lead to a better agreement between the experimental and simulated current profiles. The LH spectrum broadening caused by wave scattering is related to LH wave and plasma parameters in the edge region. However, possible influence factors and the trends of wave spectrum broadening under different LH wave parameters and plasma parameters need to be studied. In our previous work, the probability distributions of $N_{\parallel}$ and N_{θ} at the LCFS using different LH wave conditions have been studied with the LH_scatter module[25], which is based on LH propagation model[26, 27] and Bonoli and Ott's model[13, 14]. LH_scatter module was used to analyze the broadening of the LH wave spectrum caused by the interaction between LH wave and density fluctuations in SOL[25]. The previous results have shown that frequency and initial $N_{\parallel}$ can greatly broaden the probability distribution of N_{θ}, while there is a little broadening in $N_{\parallel}$ spectrum. It was further found that the N_{θ} spectrum broadening evaluated at the LCFS broadened LH wave driven current density profile, and the hard x-ray count (HXR) is more consistent with the experimental result than in the case of no scattering event ($N_{\theta} = 0$).

In this paper, the LH_scatter module is used to study the effects of plasma density parameters, namely plasma density and density fluctuation scattering length, on scattering. he total probability of scattering ($p = \sum_{\sigma} \int_{\pi}^{-\pi} d\beta\left(\Delta t P^{\sigma}(\beta)\right)$) is determined by time interval Δt (analyzed in the previous work[25]) and the scattering of probability $P^{\sigma}(\beta)$ by an angle between β and $\beta + d\beta$, in which:

$$P^{\sigma}(\beta) = \sum_{\sigma} \frac{2k_{\perp}^{\sigma}\langle(\delta n/n)^2\rangle}{V_{g\perp}^{\sigma}(\partial\varepsilon/\partial\omega)^2\xi_0^2} exp\left(-\frac{\xi^2}{\xi_0^2}\right)\left\{\left[1 + 2\frac{k_{\perp}^{\sigma 2}}{k_{tot}^2}\varepsilon_{\perp} sin^2\frac{\beta}{2}\right]^2 + \frac{k_{\perp}^{\sigma 4}}{k_{tot}^4} sin^2\beta\varepsilon_{xy}^2\right\} \quad (1)$$

Where σ refers to slow wave or fast wave, k is LH wave number, $\xi_0 = 2\pi/\lambda_c$ depends on the fluctuation correlation length (λ_c) of density fluctuation, $\varepsilon_{\parallel} = 1 - \omega_{pe}^2/\omega^2 - \omega_{pi}^2/\omega^2$, $\varepsilon_{\perp} = 1 + \omega_{pe}^2/\omega_{ce}^2 - \omega_{pi}^2/\omega^2$ and $\varepsilon_{xy} = \omega_{pe}^2/(\omega\omega_{ce})$ are dielectric tensor elements, ω_{pe}, ω_{pi} and ω_{ce} refer to electron plasma frequency, ion plasma frequency, and electron cyclotron frequency, respectively. In equation (1), the first term in the curly bracket represents the contribution of geometrical optics approximation, which ignored the effect of off-diagonal components of the lower hybrid wave dielectric tensor. The second term is formed by the coupling of the $\boldsymbol{E} \times \boldsymbol{B}$ drift produced by the lower hybrid wave with the low-frequency density perturbation.[25]

An example of a density profile and a density fluctuation profile is shown in Fig. 1 (a), which have different trends with the increase of ρ. Therefore, ρ is scanned to study the effect of density and density fluctuation on scattering. Besides, LH perpendicular wave number ($k_{\perp} = \omega N_{\perp}/c$) mainly depends on the density, and there are two different types of scattering related to $k_{\perp}$, which are large-angle scattering

($k_\perp \ll \xi_0$) near the antenna and small-angle scattering ($k_\perp \gg \xi_0$) near the LCFS[12]. In addition, fluctuation correlation length (λ_c) are varied in the model to study the effect of density fluctuation on N_θ spectrum broadening, and how N_θ spectrum broadening further affects LHCD will also be studied. The WKB approximation[22, 28, 29] is strict in the SOL, meaning it needs to be verified. The specific expression can be written as follows:

$$\left|\frac{N_\perp^2}{N^2-\varepsilon_\perp}\varepsilon_{xy}+i\frac{N_\parallel^2 N_\perp^2}{(N_\perp^2-\varepsilon_\parallel)^2}(\varepsilon_\parallel-1)\right|\frac{1}{k_\perp L}\ll 1 \tag{2}$$

where L is the scale length of equilibrium variations ($L=(|\nabla n_e/n_e|)^{-1}=\lambda_{ne}$, where λ_{ne} is the density decay length). The detailed derivation process is given in Biswas's paper.[22] The region satisfying WKB approximation can be shown in Fig. 1 (b). The position of the antenna in EAST is about $\rho\approx 1.15$. It is assumed that the slow wave is launched from the position of $\rho=1.12$ to satisfy WKB approximation, and the antenna-plasma coupling problem is ignored because it is difficult to distinguish from wave propagation.[30] In this condition, the dispersion tensor $|\mathbb{D}|<10^{-10}$, meaning that the dispersion relation is satisfied[31].

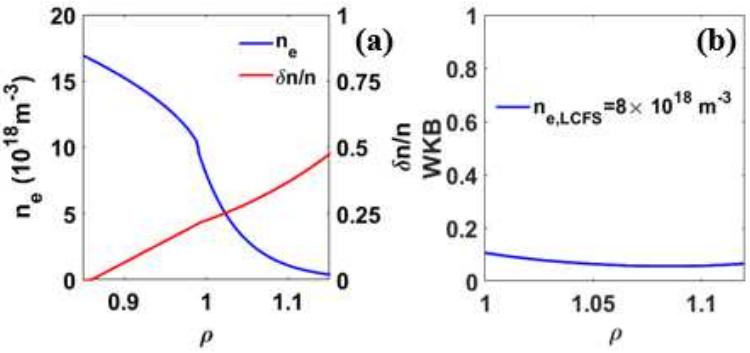

Fig. 1 (a) Density and density fluctuation profile; (b) WKB approach validation in SOL with $\lambda_{ne}=0.05$, $N_\parallel=-2.23$ and $f_{LH}=2.45\ GHz$

Based on density and density fluctuation profiles in Fig. 1 (a), the comparison of total scattering probability distribution, the contributions of both the geometrical optics approximation term and the $\boldsymbol{E}\times\boldsymbol{B}$ drift term to the distributions of scattering probability and scattering angle under different ρ are calculated as shown in Fig. 2. It is clear that the total scattering probability increases first and then decreases as the wave propagates to smaller ρ, which means that the total scattering probability has a maximum at a certain radial position (ρ_{opt}). Therefore, the total scattering probability is formed by density and density fluctuation together. As shown in equation (1), when $\lambda_c=1\ cm$ is fixed, density fluctuation affects the magnitude of total scattering probability only, but density affects both the magnitude and shape of total scattering probability by two aspects, one is the geometrical optics approximation term, which is higher and has a smaller half-width in the case of small ρ; the other is the $\boldsymbol{E}\times\boldsymbol{B}$ drift term with two peaks, which is proportional to n_e^2 ($\varepsilon_{xy}^2\propto n_e^2$). According to the

scattering module, the scope of scattering angle can be calculated by $cos\beta = 1 - \xi_0^2/k_\perp^2$, meaning that a high density makes a narrow scope of scattering angle. In general, the effect of density on total scattering probability is mainly reflected in the intensity and proportion of the geometrical optics approximation term and $\boldsymbol{E} \times \boldsymbol{B}$ drift term. With the decrease of ρ, the proportion of $\boldsymbol{E} \times \boldsymbol{B}$ drift term is larger and larger, while the proportion of geometrical optics approximation term is smaller and smaller.

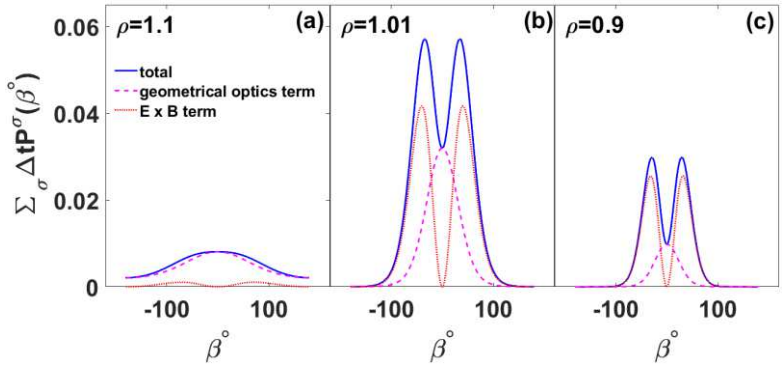

Fig. 2 Comparison of scattering probability at different ρ, where the y-axis is the total probability of scattering by an angle between β and $\beta + d\beta$. The solid blue line refers to total scattering probability, the pink dashed line refers to the contribution of geometrical optics approximation term, and the red dotted line refers to the contribution of $\boldsymbol{E} \times \boldsymbol{B}$ drift term. (a) $\rho = 1.1$; (b) $\rho = 1.01$; (c) $\rho = 0.9$

In addition to density, density fluctuation parameters are also an important factor in affecting wave scattering. According to equation (1), density fluctuation level only affects total scattering probability but doesn't affect scattering angle. As shown in Fig. 1 (a) and Fig. 2, the normalized density fluctuation level decreases at smaller ρ, but the total scattering probability increases first and then decreases, indicating that density fluctuation level and density jointly determine the scattering probability. Regardless of density fluctuation level, the impact of fluctuation correlation length on the scattering probability distribution and the N_θ spectrum broadening is studied. And further the N_θ spectrum broadening under different λ_c is used in GENRAY/CQL3D[32, 33] ray-tracing/Fokker-Planck code package to study the effect of scattering on LHCD. In order to facilitate the combination with GENRAY/CQL3D, the impact of density fluctuation within the LCFS is ignored. Based on density and density profiles shown in Fig .1 (a), the comparison of scattering probability distribution and spectrum distribution under different λ_c are shown in Fig. 3, indicating that the scattering angle distribution is clearly modified by λ_c. A smaller λ_c leads to a larger scattering angle, and the contribution of the $\boldsymbol{E} \times \boldsymbol{B}$ drift term is more important than that of the geometrical optics approximation term. It means that λ_c does not affect total scattering probability significantly but affects scattering angle distribution greatly, as shown in Fig 3 (a). As seen from Fig. 3 (b), the $N_\parallel$ probability distribution at the LCFS, which is formed by the accumulation of all scattering events on the ray trajectory from the antenna to the LCFS, is broadening a little in both λ_c case. While N_θ probability distribution at the LCFS is much flatter at small λ_c than that at large λ_c due to the larger scattering angle probability in the case of small λ_c, as shown in Fig. 3 (c).

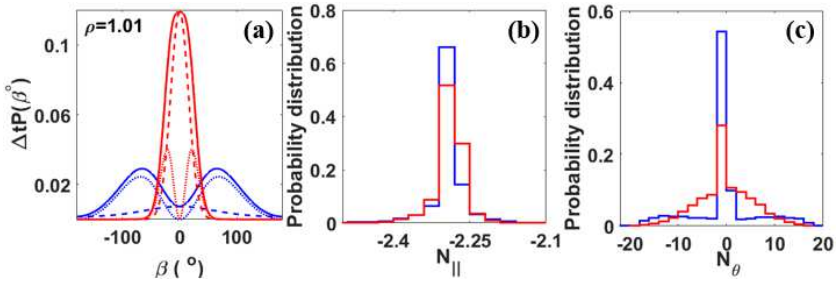

Fig. 3 (a) Scattering probability distribution over β under different λ_c, the blue line refers to $\lambda_c = 0.5\ cm$ and red line refers to $\lambda_c = 2\ cm$; the type of lines is the same as Fig. 2; (b) $N_{\|}$ probability distribution at the LCFS under different λ_c; (c) N_θ probability distribution at the LCFS under different λ_c

As the $N_{\|}$ spectrum broadening caused by scattering is too small to modify ray trajectory and LHCD[23], only the influence of different N_θ spectrum distributions at the LCFS on LHCD is considered. Two different N_θ spectrum distributions shown in Fig. 3 (c) are used as initial input to the GENRAY/CQL3D, in which all conditions are the same (B_t=2.5 T, I_p=500 kA, $\bar{n}_e = 3.5 \times 10^{19}\mathrm{m}^{-3}$, $n_{e,LCFS} = 8 \times 10^{18}\mathrm{m}^{-3}$, T_{e0}=1.3 keV, $T_{e,LCFS}$=12 eV, $V_{loop} \neq 0$, $P_{LH} = 1$ MW) except the N_θ spectrum input to GENRAY. Besides, proper evolution of the electron distribution requires taking small time steps in CQL3D[19, 22, 23], which is taken between turbulence turnover time ($\tau_f = 10^{-5}s$) and fast ekectron slowing-down time ($\tau_{fsd} \sim 10^{-3}s$). Simulated LH driven current density profiles are shown in Fig. 4, which indicates that the change in the initial N_θ spectrum distribution at the LCFS has a significant effect on LHCD, and scattering may make LH drive current density profile larger and more inward in this case.

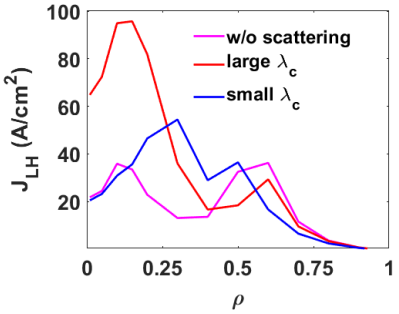

Fig. 4. Simulated LH-driven current density profile; the pink line refers to no scattering case ($N_\theta = 0$) with $I_{LH} = 150.3kA$, the red lines refer to scattering case under $\lambda_c = 2cm$ with $I_{LH} = 176.5kA$ and the blue lines refer to scattering case under $\lambda_c = 0.5cm$ with $I_{LH} = 164.7kA$

In summary, plasma density parameters can greatly influence scattering, which is mainly reflected in the following aspects. Firstly, the total scattering probability increases first and then decreases with the decrease of ρ, because the total scattering probability mainly depends on the density and density fluctuation together by changing the intensity and a proportion of geometrical optics approximation term and the $\boldsymbol{E} \times \boldsymbol{B}$ drift term. Secondly, density plays an important role in determining the magnitude and shape of the total scattering probability distribution. The higher density leads to higher scattering probability and the narrower scattering angle, as the $\boldsymbol{E} \times \boldsymbol{B}$ drift term is proportional to n_e^2. Thirdly, the effect of density fluctuation on the

spectral distribution shape mainly comes from the fluctuation correlation length rather than the density fluctuation level in the SOL. The fluctuation correlation length can flatten the scattering angle distribution to a great extent since the $\boldsymbol{E} \times \boldsymbol{B}$ drift term is dominant in a small fluctuation correlation length. Finally, the N_θ spectrum broadening induced by scattering may help LH wave propagate and damp closer to the core, which is consistent with the result on Alcator C-Mod[18] and Tore Supra[19]. In addition, some questions need to be studied in future, such as the density fluctuation affected by LH wave[34] and multi-pass absorption with edge reflections[35], which may be enhance wave scattering and make the N_θ spectrum wider[25]. And the power absorption and transmission coefficients of LH wave in SOL are also important[20, 36], but it is difficult to deal with the effects of diffusion or interference in ray trajectory. It could be clarified by methods of full wave[15-17] or particle-in-cell (PIC) [37-40], which is still under consideration at present.

Supported by the National Key Research and Development Program of China (Grant No. 2016YFA0400603, 2016YFA0400602), the national natural science foundation of China (Grant No.11975266, 11775259, 11675214, 11805233, U19A20113). Supported by United States Department of Energy Grant number DE-SC0010492. We would like to thank Dr. P. T. Bonoli for several useful discussions concerning the scattering model formulated in Ref. [14].

The authors have no conflicts to disclose.

DATA AVAILABILITY

The data that support the findings of this study are available from the corresponding author upon reasonable request.

1. N. J. Fisch, Phys Rev Lett **41** (13), 873-876 (1978).
2. W. A. Houlberg, C. Gormezano, J. F. Artaud, E. Barbato, V. Basiuk, A. Becoulet, P. Bonoli, R. V. Budny, L. G. Eriksson, D. Farina, Y. Gribov, R. W. Harvey, J. Hobirk, F. Imbeaux, C. E. Kessel, V. Leonov, M. Murakami, A. Polevoi, E. Poli, R. Prater, H. S. John, F. Volpe, E. Westerhof, A. Zvonkov, I. S. S. O. T. Group, I. C. D. Group and Model, Nucl Fusion **45** (11), 1309-1320 (2005).
3. J. Garcia, G. Giruzzi, J. F. Artaud, V. Basiuk, J. Decker, F. Imbeaux, Y. Peysson and M. Schneider, Phys Rev Lett **100** (25), 255004 (2008).
4. R. J. La Haye, Phys Plasmas **13** (5) (2006).
5. G. M. Wallace, R. R. Parker, P. T. Bonoli, A. E. Hubbard, J. W. Hughes, B. L. LaBombard, O. Meneghini, A. E. Schmidt, S. Shiraiwa, D. G. Whyte, J. C. Wright, S. J. Wukitch, R. W. Harvey, A. P. Smirnov and J. R. Wilson, Phys Plasmas **17** (8), 082508 (2010).

6. R. Cesario, L. Amicucci, A. Cardinali, C. Castaldo, M. Marinucci, L. Panaccione, F. Santini, O. Tudisco, M. L. Apicella, G. Calabro, C. Cianfarani, D. Frigione, A. Galli, G. Mazzitelli, C. Mazzotta, V. Pericoli, G. Schettini, A. A. Tuccillo, B. Angelini, G. Apruzzese, E. Barbato, G. Belli, W. Bin, L. Boncagni, A. Botrugno, S. Briguglio, A. Bruschi, S. Ceccuzzi, C. Centioli, S. Cirant, F. Crisanti, O. D'Arcangelo, R. De Angelis, L. Di Matteo, C. Di Troia, B. Esposito, G. Fogaccia, V. Fusco, L. Gabellieri, A. Garavaglia, E. Giovannozzi, G. Granucci, G. Grossetti, G. Grosso, F. Iannone, G. Maddaluno, D. Marocco, P. Micozzi, A. Milovanov, F. Mirizzi, G. Monari, A. Moro, S. Novak, F. P. Orsitto, M. Panella, G. Pucella, G. Ravera, E. Sternini, E. Vitale, G. Vlad, V. Zanza, M. Zerbini, F. Zonca and F. Team, Nat Commun **1** (2010).
7. J. P. Bizarro, J. S. Ferreira, P. Rodrigues, R. Arslanbekov and Y. Peysson, Phys Rev Lett **75** (20), 3780-3780 (1995).
8. Y. Peysson, R. Arslanbekov, V. Basiuk, J. Carrasco, X. Litaudon, D. Moreau and J. P. Bizarro, Phys Plasmas **3** (10), 3668-3688 (1996).
9. H. Takahashi, Phys Plasmas **1** (7), 2254-2276 (1994).
10. B. J. Ding, M. H. Li, Y. C. Li, R. Cesario, A. A. Tuccillo, R. Parker, S. G. Baek, Y. F. Wang, H. Q. Liu, J. C. Xu, M. Wang, H. C. Hu, C. B. Wu, L. Wang, H. Lian, S. Y. Lin, Y. Liu, H. L. Zhao, J. F. Shan, F. K. Liu, J. P. Qian, X. Z. Gong, J. G. Li and B. N. Wan, Nucl Fusion **58** (12), 126015 (2018).
11. P. M. Bellan and K. L. Wong, Phys Fluids **21** (4), 592-599 (1978).
12. P. L. Andrews and F. W. Perkins, Phys Fluids **26** (9), 2537-2545 (1983).
13. E. Ott, Phys Fluids **22** (9), 1732-1736 (1979).
14. P. T. Bonoli, Phys Fluids **25** (2), 359-375 (1982).
15. M. Madi, Y. Peysson, J. Decker and K. Y. Kabalan, Plasma Phys Contr F **57** (12), 125001 (2015).
16. C. Lau, E. H. Martin, S. Shiraiwa and G. M. Wallace, Nucl Fusion **60** (3), 036001 (2020).
17. A. K. Ram and K. Hizanidis, Phys Plasmas **23** (2), 022504 (2016).
18. N. Bertelli, G. Wallace, P. T. Bonoli, R. W. Harvey, A. P. Smirnov, S. G. Baek, R. R. Parker, C. K. Phillips, E. J. Valeo, J. R. Wilson and J. C. Wright, Plasma Phys Contr F **55** (7), 074003 (2013).
19. Y. Peysson, J. Decker, L. Morini and S. Coda, Plasma Phys Contr F **53** (12), 124028 (2011).
20. V. P. Ridolfini, M. L. Apicella, G. Calabro, C. Cianfarani, E. Giovannozzi and L. Panaccione, Nucl Fusion **51** (11), 113023 (2011).
21. S. G. Baek, B. Biswas, P. T. Bonoli, D. Brunner, I. C. Faust, A. E. Hubbard, J. W. Hughes, B. LaBombard, R. T. Mumgaard, M. Porkolab, S. Shiraiwa, G. M. Wallace and S. J. Wukitch, AIP Conference Proceedings **2260**, 030006 (2020).
22. B. Biswas, S. Gyou Baek, P. Bonoli, S. i. Shiraiwa, G. Wallace and A. White, Plasma Phys Contr F **62** (11), 115006 (2020).
23. J. Decker, Y. Peysson, J. F. Artaud, E. Nilsson, A. Ekedahl, M. Goniche, J. Hillairet and D. Mazon, Phys Plasmas **21** (9), 092504 (2014).

24. S. G. Baek, B. Biswas, G. M. Wallace, P. T. Bonoli, B. J. Ding, M. H. Li, Y. C. Li, Y. F. Wang, M. Wang, C. B. Wu, G. H. Yan, J. Chen, X. Zhai, A. M. Garofalo, W. Choi, F. Poli and S. Shiraiwa, Nucl Fusion **61** (10) (2021).
25. C. B. Wu, B. J. Ding, M. H. Li, S. G. Baek, G. M. Wallace, Y. C. Li, G. H. Yan and S. C. Liu, Phys Plasmas **28** (8) (2021).
26. S. Weinberg, Physical Review **126** (6), 1899-1909 (1962).
27. T. H. Stix, The Theory of Plasma Waves (1962).
28. A. Cardinali, L. Morini, C. Castaldo, R. Cesario and F. Zonca, Phys Plasmas **14** (11), 112506 (2007).
29. A. Cardinali and F. Santini, Plasma Phys Contr F **53** (12), 125001 (2011).
30. M. Brambilla, Nucl Fusion **19** (10), 1343-1357 (1979).
31. Y. Peysson and J. Decker, EUR-CEA-FC-1739 (2008).
32. A. P. Smirnov and R. Harvey, Bull. Am. Phys. Soc. **40**, 1837 (1995).
33. W. Harvey and M. McCoy, Proc. IAEA Technical Committee Meeting on Simulation and Modeling of Thermonuclear Plasmas (1992).
34. R. Cesario, L. Amicucci, A. Cardinali, C. Castaldo, M. Marinucci, F. Napoli, F. Paoletti, D. De Arcangelis, M. Ferrari, A. Galli, G. Gallo, E. Pullara, G. Schettini and A. A. Tuccillo, Nucl Fusion **54** (4), 043002 (2014).
35. V. Fuchs, P. T. Bonoli, I. P. Shkarofsky, A. Cote, Y. Demers and C. Janicki, Nucl Fusion **35** (1), 1-22 (1995).
36. V. PericoliRidolfini, A. Ekedahl, Y. Baranov, J. A. Dobbing, B. Fischer, C. Gormezano, M. Lennholm, F. Rimini, J. Romero, P. Schild and F. X. Soldner, Plasma Phys Contr F **39** (7), 1115-1128 (1997).
37. A. Kuley, Z. X. Wang, Z. Lin and F. Wessel, Phys Plasmas **20** (10) (2013).
38. J. Bao, Z. Lin, A. Kuley and Z. X. Wang, Nucl Fusion **56** (6) (2016).
39. T. G. Jenkins, T. M. Austin, D. N. Smithe, J. Loverich and A. H. Hakim, Phys Plasmas **20** (1) (2013).
40. A. Kuley, Z. Lin, J. Bao, X. S. Wei, Y. Xiao, W. Zhang, G. Y. Sun and N. J. Fisch, Phys Plasmas **22** (10) (2015).